Supplementary Materials for

Structural Basis for Cloverleaf RNA-initiated Viral Genome Replication

Keerthi Gottipati[1,2 #], Sean C. McNeme[1 #], Jerricho Tipo[1], Mark A. White [1], and Kyung H. Choi[1,2 *]

[1] Department of Biochemistry and Molecular Biology, Sealy Center for Structural Biology and Molecular Biophysics, University of Texas Medical Branch, 301 University Boulevard, Galveston, Texas, USA.

[2] Department of Molecular and Cellular Biochemistry, Indiana University, 212 S. Hawthorne Drive, Bloomington, Indiana, USA

[#]These authors contributed equally to this work

*Corresponding author: kaychoi@iu.edu

This file includes:

Figs. S1 to S4

Table S1

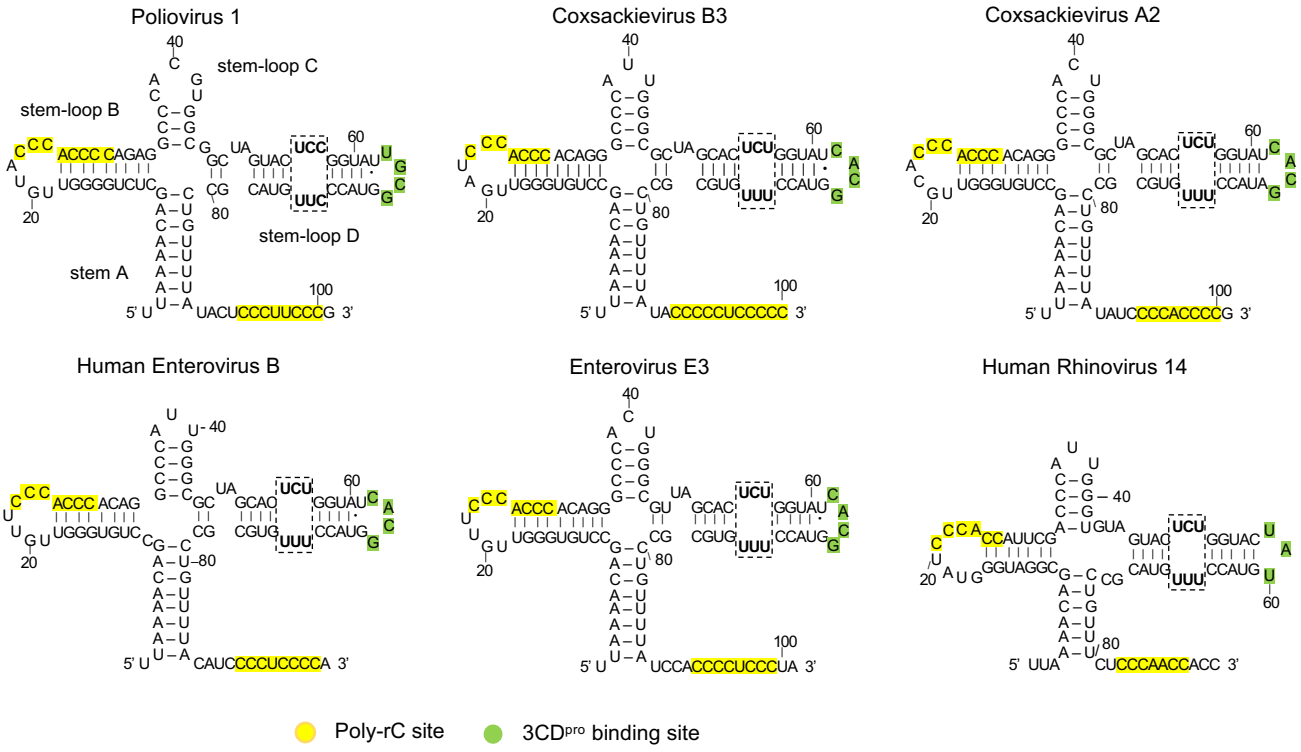

Fig. S1. Predicted secondary structures of enteroviral cloverleaf RNAs. Secondary structures of poliovirus 1 (Genbank accession no. V01149.1), coxsackievirus B3 (AY752944.2), coxsackievirus A2 (NC_038306.1), human enterovirus B (NC_001472.1), echovirus E3 (AB647326.1), human rhinovirus 14 (K02121.1) cloverleaf RNAs were predicted using RNAfold webserver (*54*). In some cases, the base pairing pattern of the nucleotides at the four-way junction was ambiguous. Thus, the secondary structures were modified based on the crystal structures of CVB3 and PV cloverleaf RNAs. The pyrimidine mismatch region in stem-loop D is shown in bold and boxed. The poly-rC regions in stem-loop B and 3' end are shaded in yellow, and the 3CD^{pro} binding site in stem-loop D is shaded in green.

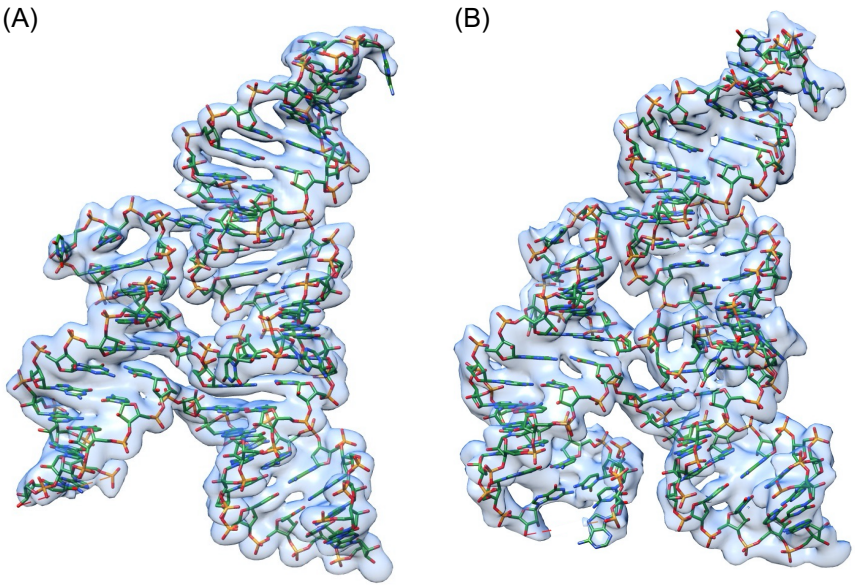

Fig. S2. Structure comparison between CVB3 and PV cloverleaf RNAs. The $2F_o$-F_c map contoured at 1.2 σ is shown along with the CVB3 cloverleaf **(A)** and PV cloverleaf **(B)** structure. For clarity, only the cloverleaf RNAs of tRNA-CL constructs are shown.

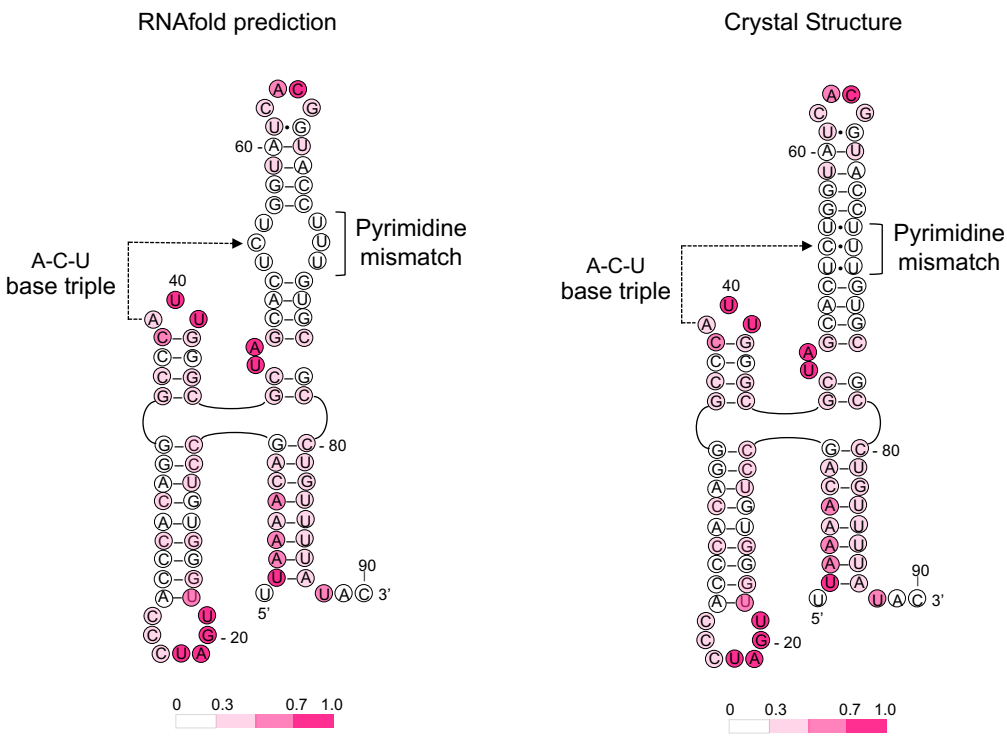

Fig. S3. Comparison of the CVB3 cloverleaf RNA structure with SHAPE data. The normalized SHAPE reactivities determined for CVB 5' UTR (*19*) are mapped on the secondary structures of CVB3 cloverleaf predicted by the RNAfold program or derived from the crystal structure. The positions of the A•C-U base triple and pyrimidine mismatch are indicated. The pyrimidine mismatch does not show high SHAPE reactivity expected from the secondary structure prediction. Instead, the nucleotides in pyrimidine mismatch form non-Watson-Crick base pairs in the crystal structure, consistent with low reactivity in SHAPE analysis. A39 in the apical loop of stem-loop C also has relatively low SHAPE reactivity, consistent with the A•C-U base triple formation.

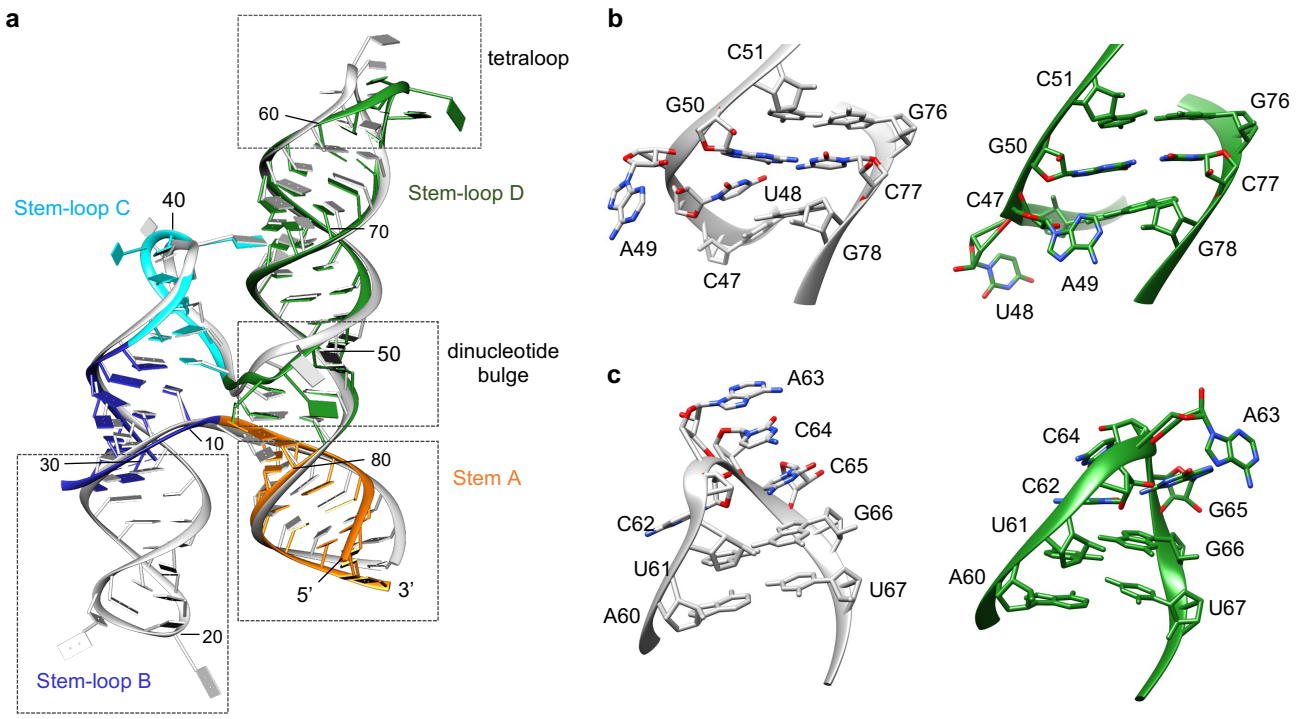

Fig S4. Comparison of CVB3 cloverleaf structures. **a**. Superposition of the CVB3 cloverleaf RNA structures determined using the tRNA and Fab scaffolds. The current structure is colored as in Fig 1 and the Fab-bound structure (Das et al.) is colored in white. The tRNA and Fab scaffold structures were removed for clarity. Dashed boxes highlight the areas of major differences in the two structures. **b**. Comparison of the ^{48}UA^{49} dinucleotide bulge structures. In our structure, U^{48} and A^{49} are flipped out of stem D, leaving the RNA double helix unperturbed. In the Fab-bound structure, A^{49} is flipped out and interacts with a neighboring Fab molecule, while U^{48} hydrogen bonds with the G^{50} and C^{77} base pair within the RNA helix. This locally disrupts the helical stacking. **c**. Comparison of the tetraloop structures in stem-loop D. The Fab-bound structure contains G65C mutation, and the resulting tetraloop (^{62}CACC^{65}, WT cloverleaf numbering) forms a GNRA-type motif. A^{63} and C^{64} are solvent exposed and cap the end of the loop. In our structure, the ^{62}CACG^{65} tetraloop forms a UNCG-type motif, where C^{62} forms stabilizing hydrogen bonds with G^{65}, while A^{63} and C^{64} cap the loop and interact with the solvent on either side of the tetraloop.

Table S1. Summary of ITC derived thermodynamic parameters for the binding between PCBP2 domains and PV cloverleaf RNA constructs.

PCPB2 domains	PV RNA*	Kd (μM)**	ΔH (kcal·mol^{-1})	-TΔS (kcal·mol^{-1})	n (sites)
KH1/2	Stem-loop B	22.9 ± 6.3	-8.6 ± 1.64	2.40	0.60
	WT cloverleaf (tRNA-CL^{WT})	30.7 ± 12.3	-18.2 ± 10.76	12.52	0.83
	A39U cloverleaf (tRNA-CL^{A39U})	20.8 ± 6.1	-10.4 ± 1.9	4.43	0.71
	3' Poly-rC	1.7 ± 0.23	-12.4 ± 0.39	5.03	0.93
KH3	Stem-loop B	2.4 ± 0.30	-7.8 ± 0.24	0.60	0.65
	WT cloverleaf (tRNA-CL^{WT})	14.8 ± 3.3	-11.2 ± 2.46	5.05	0.60
	A39U cloverleaf (tRNA-CL^{A39U})	5.0 ± 0.45	-14.7 ± 0.34	7.96	0.88
	3' Poly-rC	1.1 ± 0.09	-19.7 ± 0.29	12.1	0.33

*Binding interactions were measured at 4 °C with synthetic RNAs, stem-loop B and 3'poly-rC site, and wild-type and A39U mutant cloverleaf, tRNA-CL^{WT} and tRNA-CL^{A39U}.

**The values are an average of at least two independent measurements ± error propagated from individual fits.